UDC 524.3
IRSTI 41.25.29

https://doi.org/10.55452/1998-6688-2026-23-1-346-357

[1,2]Alimgazinova N.Sh.,
Cand. Phys.-Math. Sc., ORCID ID: 0000-0002-4596-1855
e-mail: Nazgul.Alimgazinova@kaznu.kz
[2,3]Manapbayeva A.B.,
PhD, ORCID ID: 0000-0002-0322-1509
e-mail: manapbayeva.arailym@gmail.com
[1,2]*Omar A.Zh.,
PhD, ORCID ID: 0000-0002-5604-3742
*e-mail: omaruzhan@gmail.com
[1,2]Demessinova A.M.,
PhD, ORCID ID: 0000-0001-5049-9338
e-mail:aizat.dem@gmail.com
[1,2]Turekhanova K.M.,
Cand. Phys.-Math. Sc., ORCID ID: 0000-0003-4662-7290
e-mail: kunduz@physics.kz
[1]Abildayev N.E.
ORCID ID: 0009-0009-1934-4907
e-mail: nurlanabildaev833@gmail.com.

[1]Al-Farabi Kazakh National University, Almaty, Kazakhstan,
[2]Institute of Experimental and Theoretical Physics,
Al-Farabi Kazakh National University, Almaty, Kazakhstan,
[3]Kazakh National Women's Teacher Training University, Almaty, Kazakhstan,

STUDY OF THE W40 STAR-FORMING REGION BASED ON OBSERVATIONS BY THE WISE INFRARED SPACE TELESCOPE

Abstract

The study of the mechanisms of star formation and evolution is based on comprehensive research into interstellar regions, including the analysis and identification of young stellar objects (YSOs). The identification of young stellar objects by their radiation at various wavelengths in the infrared range is a relatively recent development - the first studies in this field appeared only at the end of the 20th century. The development of this field has been made possible by improvements in observation techniques and data processing methods, the acquisition of more reliable characteristics of stellar sources, and the creation of catalogs containing extensive arrays of information about cosmic objects. In this study, the star-forming region W40 of the Aquilla molecular cloud was investigated in the infrared wavelength range to detect previously unidentified young stellar objects at various stages of evolution. Identification was carried out using two approaches: photometric criteria and spectral indices. This made it possible to more reliably identify the evolutionary stages of 37 newly discovered and previously unexplored YSO candidates (5 objects of class I, 2 objects of class II, 4 objects – class "transitional disks" and 26 objects — class III), which indicates an active and ongoing process of star formation in W40.

Keywords: W40 star-forming region, infrared radiation, wise, young stellar objects (yso), evolutionary stage.

Received: November 27, 2025; accepted: March 12, 2026.

Introduction

The identification of young stellar objects based on their radiation at various wavelengths in the infrared range is a relatively recent development, with the first studies appearing only at the end of the 20th century. The development of this field has been made possible by improvements in observation techniques and methods, the emergence of more reliable data on stellar objects and the creation of catalogs containing extensive arrays of information about cosmic objects.

Early studies on identifying young stellar objects (YSOs) were based on analyzing the energy distribution in spectra (EDS) [1]. Later, criteria based on radiation fluxes in the near- and mid-infrared ranges obtained from the 2MASS ground-based survey and observations by the Spitzer, WISE, and Herschel space telescopes began to be widely used for this purpose. Currently, YSO identification algorithms based on established infrared color–color and color–magnitude selection criteria are actively applied [2–5].

However, there is still no universal method that fully satisfies all identification criteria applicable to various observational data. Based on previous studies of other regions of the interstellar medium, various identification methods were applied to determine the true YSOs in the W40 star-forming region [6-9].

The Aquila molecular cloud, or Aquila Rift complex, is an area of the sky located in the constellations Aquila, Serpens Cauda and Ophiuchus and includes dark interstellar clouds. The Aquila Rift forms an elongated structure oriented from northeast to southwest. This region is part of the Great Rift, the closest dark cloud of interstellar dust to us, which obscures the central part of the Milky Way's galactic plane, extending towards its inner and radial sectors.

Numerous star-forming regions have been discovered in the Aquila cloud complex, grouped into two main zones: Aquila-North (within galactic coordinates for latitude b from 2° to -6° and longitude l from 29° to -34°) and Aquila-South (galactic latitude b occupies the region from 2° to -5° and longitude l from 26° to -30°) [10]. In the northern part of the complex, Aquila-North, the Serpens Main and Serpens B clusters stand out [11–13]. The southern region, Aquila-South, is characterized by the presence of three key star-forming centers: Serpens South, W40 and MWC297 [12, 13].

Determining the distance to the Aquila cluster has been the subject of numerous early studies, but these works showed significant discrepancies [13–16]. For example, the stellar photometry method in study yielded an estimate of about 255 pc, while X-ray analysis and HR diagram analysis indicated a distance of more than 350 pc [12, 17]. Significant progress was made thanks to VLBI observations, which made it possible to measure the parallaxes of stars in Serpens Main and obtain a distance of about 415 pc [18]. In subsequent years, with the development of VLBI and the emergence of data from the Gaia mission, it became possible to take measurements at even greater distances with higher accuracy. In particular, Gould's Belt used 8 years of VLBI data to demonstrate that individual clouds, such as Serpens Main, W40 and Serpens South, are physically connected and form a single cloud structure at an average distance of 436±9 pc [19]. The VLBI distances obtained are also confirmed by later Gaia data [20, 21].

During the Gould's Belt study, the Aquila complex was surveyed using the Herschel telescope [22]. The survey covered an area of 3.30×3.30 angular degrees and included the creation of maps in the far-infrared range. These maps, obtained in five bands from 70 to 500 μm, had high spatial resolution and sensitivity. For data analysis, dust thermal radiation was modeled using a modified blackbody function, which allowed for the creation of column density and temperature maps. Figure 1 shows a dust temperature map for the Aquila region. Analysis of the map showed that areas where stars are actively forming, such as Serpens Main, Serpens B, and Serpens South, are characterized by high dust density and relatively low temperatures. At the same time, in the more developed HII W40 region, the dust temperature was higher than in the surrounding areas. The study revealed many new protostars and pre-stellar cores concentrated in three main star-forming regions: a filamentary molecular cloud centered on Serpens South, the eastern part of HII W40/Sh2-64 and the MWC 297/Sh2-62 region located to the south.

W40 is a young star cluster closely associated with an HII region [25, 26]. This cluster, formed in a giant molecular cloud with a mass of about 1.4×10^5 solar masses, is surrounded by a diffuse nebula consisting of interstellar gas [27–29]. Most of this gas was scattered during the process of star formation. The massive OB stars born in W40 ionized the surrounding gas, forming an hourglass-shaped HII region. Due to the strong absorption of light by the dust of the molecular cloud, W40 is not accessible for observations in the visible range. Therefore, X-ray, infrared and radio observations are used to study star formation processes in this region, located at a distance of 1420 ± 30 light-years and one of the closest sites of massive O and B star formation. In particular, observations of ammonia (NH_3) emission are widely used to trace dense molecular gas and to investigate the temperature and kinematic structure of star-forming regions such as W40 [30, 31].

Thus, studying the W40 star-forming region of the Aquila Rift complex across a wide range of wavelengths and using a variety of methods could become an important research area in the study of the early stages of star formation on a large scale.

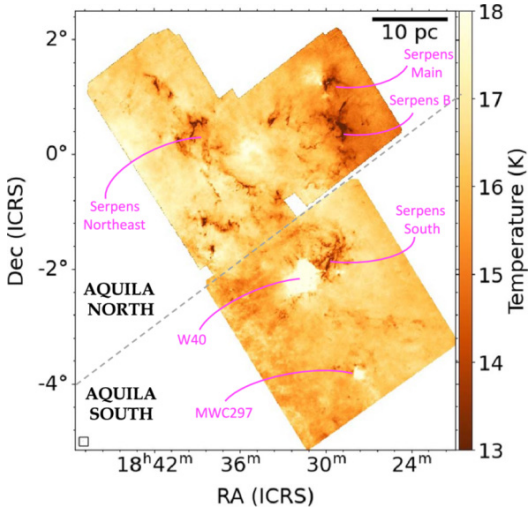

Figure 1 – Dust temperature map of the Aquila molecular clouds obtained using the Herschel telescope [23]

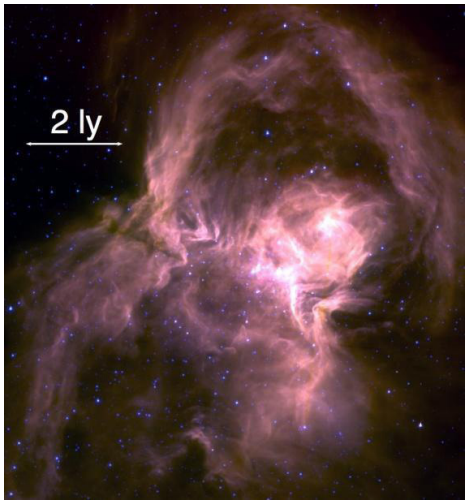

Figure 2 – Image of the W40 star-forming region obtained by the Spitzer Space Observatory [24]

Materials and methods

An analysis of the literature on the W40 star-forming region allowed the determination of its central coordinates and angular dimensions. Based on these data, the search radius for young stellar objects (YSOs) relevant to this study was established. For the W40 H II region, with apparent dimensions of 17′ × 30′, the equatorial coordinates of the center are RA (J2000) = $18^h31^m29^s$ and Dec (J2000) = −02°05′36 [31]″.

This study used data from large-scale infrared surveys 2MASS and WISE (Wide-Field Infrared Survey Explorer). Near-infrared observations in the J (1.25 μm), H (1.65 μm), and Ks (2.17 μm) bands obtained by 2MASS are presented in the 2MASS All-Sky Point Source Catalog [32]. WISE survey data are included in the AllWISE catalog, which provides flux measurements in the W1 (3.4 μm), W2 (4.6 μm), W3 (12 μm), and W4 (22 μm) bands [33].

Summary information on the region and the infrared sources detected within the specified radius is given in Table 1.

To conduct this study, it was necessary to exclude false infrared sources, so objects were selected from the above-mentioned catalogs that contained reliable non-zero radiation fluxes, with a flux error not exceeding 0.2 mag. In addition, considering that in the AllWISE catalog, sources with a signal-to-noise ratio higher than 3 have a quality flag of A or B, objects corresponding to this criterion were selected.

However, as noted, some of the objects selected based on flux quality criteria may be “false” sources, mainly associated with the radiation of interstellar medium structures [34]. The exclusion of such objects is crucial for the correct determination of the number of YSOs associated with star-forming regions. Therefore, all infrared sources were additionally subjected to visual inspection. The analysis was performed on both single-band images in the W3 band (12 μm) and composite images of three WISE bands (W1, W2, W3). An infrared source was classified as “fake” if there was no distinct point object in the W3 image corresponding to the source observed in the W1 and W2 images. As expected, most of the false sources were associated with gradients or diffuse radiation structures at a wavelength of 12 μm.

Table 1 – Object search parameters

Region	R.A. Range (deg)	Decl. Range (deg)	Search radius (arcmin)	Number of objects found
W40	277.73 ≤α≤278.00	-02.095≤δ≤-02.107	8	773

Results and discussion

First and foremost, for the purpose of this study, we excluded infrared sources that could mimic YSO signals, even though they are not genuine YSOs. To filter out such contaminants, we employed a methodology similar to that described, applying the criteria outlined in [35, 36].

Sources associated with galaxies exhibiting active star formation were first excluded. These galaxies are characterized by strong emission from polycyclic aromatic hydrocarbons (PAHs), produced when hydrogen interacts with cosmic dust in evolved stars. PAH radiation from these galaxies has a pronounced red tint (for example, the color index W23 = W2–W3 demonstrates a large value) and as a rule, weaker than that of typical LSMAs. Active galactic nuclei (AGNs) can also act as sources of data contamination, since their radiation in the mid-infrared range is similar to that of LSMAs. However, within a distance of about 5 kpc from us, AGN radiation is generally weaker than that of typical LSMAs. Since our study area is located at a distance of less than 1 kpc, this factor becomes critically important for our sample. In addition to the above, infrared radiation can also be generated by charged particles at shock wave fronts and polycyclic aromatic hydrocarbons (PAHs) in the interstellar medium. Thus, all possible contaminants that are not stellar objects were excluded.

An algorithm based on the methodology described, was used to identify protostars in the W40 star-forming region [35]. Young stars were classified according to their evolutionary stages: class 0 (protostars), classes I and II, transitional disks, and class III. Class 0 YSOs are the earliest class of YSO evolution, characterized by the stage of star development before the onset of thermonuclear burning. Protostars are hidden by a gas-dust shell, but actively increase their mass through accretion. Class I protostars are characterized by the presence of a massive circumstellar shell, which gradually dissipates as they evolve. In class II protostars, radiation is mainly caused by an optically thick circumstellar disk [1, 36]. Class III protostars show very weak excess infrared radiation. Often, such sources cannot be distinguished from young main sequence stars using only infrared observations. In addition to Class I–III objects, there is also a class of “transitional disks.” These are believed to be systems with a partially cleared inner disk and a massive, optically dense outer disk. The age of transitional disks has not been precisely determined, as various possible scenarios for their origin are being discussed. The most common hypothesis is that transitional disks are an intermediate stage between class II and III objects. Identification in this work was carried out in accordance with this classification.

Based on the fact that YAGs are located in the same region of the color diagram as protostars, the latter were identified using photometric criteria from sources that had previously been classified as YAG candidates. Protostars (young stellar objects of class 0) emit brighter than most galaxies, which suggests their dominant flux in the W4 band. To identify protostars by photometric criteria, conditions based on fluxes in all bands (W1, W2, W3, W4) are used.

The identification of young stellar objects of classes I and II was performed using the first three infrared bands W1, W2 and W3. Stars of these classes can also be identified using reliable non-zero fluxes in the near-infrared range based on 2MASS data [35].

To identify young stellar objects in the transition stage between classes II and III, known as "transitional disks," criteria based on data from all four bands (W1, W2, W3, and W4) were applied. Objects that do not meet the photometric criteria for protostars, class I and II objects or "transitional disks" are classified as class III objects.

All objects selected using the above algorithm were re-checked for the presence of AAG using criteria based on color indices and stellar magnitudes in all four bands of the AllWISE catalog. As a result, according to WISE and 2MASS data, the following were identified for the W40 region: 17 objects as Class I YSOs, 39 as Class II, 12 with signs of "transitional disks" and 77 as Class III.

A study of literary sources and astronomical catalogs (including SIMBAD [37] and IRSA [38]) for each identified object revealed that young stellar objects had previously been studied in the Aquila molecular cloud, particularly in the W40 region. These studies were based on data obtained from the ALMA observatory, as well as the Spitzer and Herschel space telescopes [39–43].

For region W40, out of the 17 candidates for young stellar objects of class I that we identified, 9 objects were found in astronomical catalogs and assigned the status of "Young Stellar Object Candidate." Of the 39 candidates for young stellar objects of class II that we identified: 24 objects are "Young Stellar Object Candidates," 3 objects are "Young Stellar Objects," 2 objects are designated "Star" without specifying the spectral type, 1 object is designated "Far-IR source" without specifying the evolutionary status, and 1 object is identified as "Dense Core." Thus, out of 56 Class I and II objects, we confirmed the status of 38 objects ("YSO" and "star"), while for 20 objects, the search did not yield any information regarding their evolutionary status and studies conducted. A review and search for information on candidates in the remaining classes (77 — class III, 12 — transitional disks) showed that 17 objects have the status "Young Stellar Object Candidate" and 2 objects are "Young Stellar Objects." Also, 1 object is a "Radio Source" and 3 objects are "Stars" without specifying the spectral type.

Figure 3 shows a color diagram for all YSO candidates identified in this study, taking into account objects found with known statuses of "Young Stellar Object Candidate" and "Young Stellar Object." The filled figures are newly identified YSO candidates. As can be seen from the diagram, most of the YSO candidates we identified lie in the areas of the diagram corresponding to their evolutionary class. The discrepancy in the diagram does not indicate an incorrect determination of the evolutionary stage of the YSO; it only emphasizes the importance of using various methods to identify true YSO candidates.

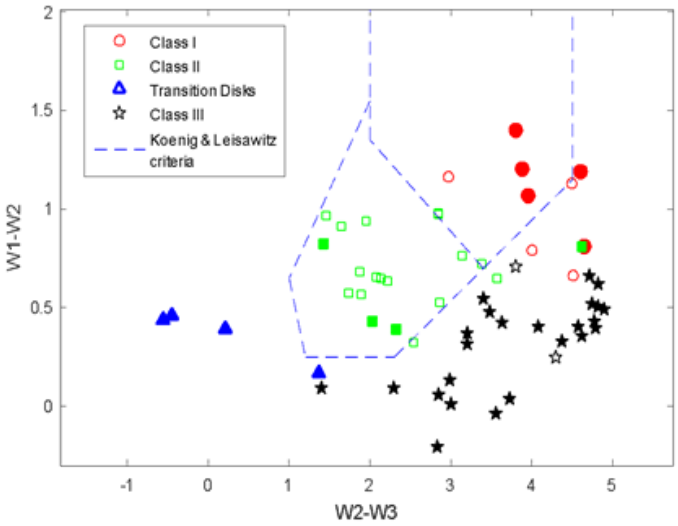

Figure 3 – Color-color diagram of candidates in the YSO

To further refine the sample and distinguish genuine YSOs from contaminants, we apply the spectral index classification criteria.

Thus, our testing based on photometric criteria of the WISE and 2MASS infrared surveys allowed us to discover 37 previously unidentified objects in the W40 region that are candidates for YSOs. Now, to identify the true YSOs, it is necessary to check them against the spectral index identification criteria.

In this classification, the YSO calculates the slope of the RES, i.e., determines the spectral index: $\alpha = d \log(\lambda F_{\lambda}) / d \log(\lambda)$. Typically, the inclination of the RES is measured between ~2 and 20 μm, since the use of mid-IR RES streams allows the IR radiation of the disk and the inner shell of the YSO to be measured. Differences in the inclination of the RES for different classes of protostars are explained by the evolution of their circumstellar environment as they age. This evolution, in turn, causes changes in the shape of their RES, manifested as infrared excesses that arise due to the presence of optically thick disks.

In the standard classification of YSOs [1], several classes are distinguished based on the slope of the RES: Class I— $\alpha \geq 0.3$; Class II— $-1.6 \leq \alpha < -0.3$; Class III — $\alpha < -1.6$ and objects with a flat spectrum — $-0.3 \leq \alpha < 0.3$. Class I MROs have an ascending or nearly flat spectrum in the wavelength range from 3 to 22 μm. Class II LEOs have a decreasing spectrum in this wavelength range. Class III LEOs exhibit very weak excess infrared radiation. Transitional disks are sources that exhibit a small excess of radiation in the near-infrared range (1–10 μm) or none at all, but have a pronounced excess in the wavelength range above 10–20 μm [44].

In this study, three methods based on the use of WISE and Spitzer flux data were applied to determine the spectral index.

For the first method, for all previously identified YSOs with values available in all four WISE bands, we used the equation for finding the spectral index according to [45]:

$$\alpha_M = 0.36(W1 - W2) + 0.58(W2 - W3) + 0.41(W3 - W4) - 2.90 \quad (1)$$

The fluxes in the bands are presented in magnitudes. The numerical coefficients are a combination of conversion factors between magnitude and flux density at the corresponding wavelengths and weighting factors. Essentially, this is a weighted average of the slopes obtained between successive pairs of WISE bands. Such a slope measurement can mitigate the effects of absorption due to nearly identical absorption coefficients across the entire WISE wavelength range, i.e.,

$$\alpha_{4.5,24} = \frac{dlog\,(\lambda F_{\lambda})}{dlog\,(\lambda)} = \frac{log\,[24F_{\lambda}(24\mu m)] - log\,[4.5F_{\lambda}(4.5\mu m)]}{log\,(24) - log\,(4.5)} \quad (2)$$

The second method for determining the spectral index is based on using only data from the two WISE bands. Since the RES between the two bands is poorly approximated by a power law, we calculate the spectral index at two endpoints by simply measuring the slope between W1 and W4 according to [34]:

$$\alpha_w = 0.488(W1 - W4) - 2.915 \quad (3)$$

In this equation, the numerical coefficients simply arise from the conversion of the required value into flux density.

To minimize attenuation effects, it is necessary to use bands centered on wavelengths greater than 4.5 μm [21]. Therefore, we applied the third method for determining the spectral index, which is based on the use of fluxes in the Spitzer/IRAC 4.5 μm and Spitzer/MIPS 24 μm bands. We determine the spectral index through the flux densities [23].

$$A_{W[1.4]} \approx 0.5\ A_k \quad (4)$$

Fluxes are expressed in mJy, and wavelengths are given in μm. For some YSO candidates, complete Spitzer measurements were not available in the catalogs, making it impossible to determine the spectral index α 4.5,24 for these sources.

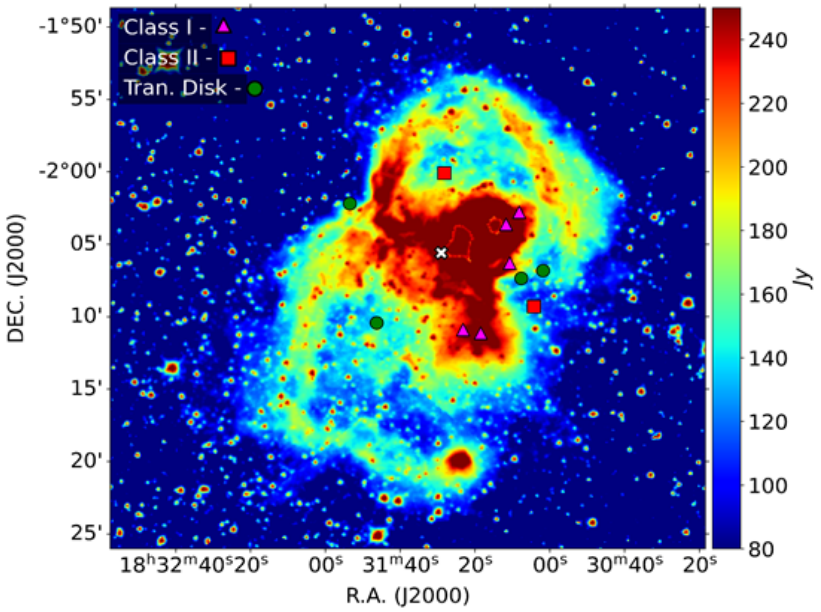

Figure 4 – Spatial distribution of early-class YSO candidates on the integrated emission intensity map of the W40 region in all four WISE bands

Based on the above classification, we determined the evolutionary stage for each previously identified candidate MZs using all three methods for determining the spectral index. Our study shows that classifying YSOs using either the spectral index or WISE colors leads to a similar selection of YSOs. For classes I and II, the stages are practically the same, while for most class III objects, we observe spectral index values corresponding to class I. Given that the Aquila molecular cloud is located near the galactic disk and based on the results, we suggest that the erroneous evolutionary stage is due to the fact that the YSOs we found are located close to the disk plane and are older objects with optically thick disks, and therefore may have Class I RES [46, 47]. This corresponds to the physical nature of Class III YSOs, as they are practically already formed young stars.

An analysis of the correspondence of evolutionary classes by object (previously identified as I, II, and transitional disks) showed that for the method of determining the spectral index based on Spitzer data, it does not exceed 23% for the W40 region, while based on WISE data, it exceeds 77%. This confirms the conclusions which also obtained a good estimate of the spectral index using WISE photometry [34]. Based on this, we selected only those objects that are well consistent with the previously specified classes. For transitional disks, we accepted the best match at a spectral index belonging to class II or III.

Figure 4 presents the spatial distribution of newly identified YSO candidates. The central coordinate of the region, used as the reference for the search, is marked with a white cross. Class I sources are shown as pink triangles, Class II sources as red squares, and transitional disks as green circles.

Table 2 presents information on candidates for YSOs of early spectral classes (Class I – 5, Class II – 2, and “transitional disks” – 4). For Class III, only those candidates for YSOs were selected whose spectral index corresponded to the previously defined stage of evolution.

Table 2 – Candidates for early evolutionary stages of YSO

AllWISE	RAJ2000	DEJ2000	W1	W2	W3	W4	YSO
	deg	deg	mag	mag	mag	mag	
J183110.70-020618.7	277,795	–2,105	11,255	10,064	5,456	2,491	I
J183111.69-020337.8	277,799	–2,060	9,420	8,021	4,223	–3,32	I
J183123.17-021053.9	277,847	–2,182	11,136	10,323	5,673	4,842	I
J183108.18-020248.1	277,784	–2,047	11,145	10,080	6,129	1,431	I
J183118.46-021108.8	277,827	–2,186	10,371	9,171	5,283	2,762	I
J183128.17-020005.3	277,867	–2,001	10,191	9,799	7,470	3,005	II
J183104.22-020918.0	277,768	–2,155	11,366	10,54	9,113	6,059	II
J183107.63-020721.5	277,782	–2,123	8,663	8,226	8,777	4,215	Tr.D
J183146.26-021025.9	277,943	–2,174	9,379	9,211	7,848	5,836	Tr.D
J183101.78-020649.6	277,757	–2,114	9,184	8,791	8,582	4,828	Tr.D
J183153.45-020212.0	277,972	–2,037	8,436	7,980	8,435	5,230	Tr.D

Conclusion

In this work, we present the results of the search and identification of YSOs in the W40 star-forming region, part of the Aquila molecular cloud. Identification was carried out using photometric criteria and spectral indices, allowing a more reliable determination of the evolutionary stages of the newly discovered YSO candidates.

As a result, 37 previously unstudied candidates were found, indicating an active and ongoing star formation process in W40. The obtained results complement existing knowledge of the structure of the Aquila Rift complex and contribute to the understanding of the mechanisms of star formation at early evolutionary stages.

Information on funding. This research was funded by the Science Committee of the Ministry of science and Higher Education of the Republic of Kazakhstan (Grant No. AP23489575).

REFERENCES

1 Lada, C.J. Star formation: from OB associations to protostars. IAU Symposium, 115, 1–17 (1987). https://doi.org/10.1017/S0074180900094766

2 Allen, L.E., et al. Initial results from the Spitzer Young Stellar Cluster Survey. Astrophysical Journal Supplement Series, 154 (1), 367–373 (2004). https://doi.org/10.1086/422823

3 Gutermuth, R.A., et al. The Spitzer Gould Belt Survey of large nearby interstellar clouds: discovery of a dense embedded cluster in the Serpens–Aquila Rift. Astrophysical Journal, 673 (2), L151–L154 (2008). https://doi.org/10.1086/528710

4 Koenig, X.P., and Leisawitz, D.V. A classification scheme for young stellar objects using the Wide-field Infrared Survey Explorer AllWISE catalog: revealing low-density star formation in the outer Galaxy. Astrophysical Journal, 791 (2), 131 (2014). https://doi.org/10.1088/0004-637X/791/2/131

5 Fischer, W.J., et al. A WISE census of young stellar objects in Canis Major. Astrophysical Journal, 827 (2), 96 (2016). https://doi.org/10.3847/0004-637X/827/2/96

6 Manapbaeva, A.B., Esimbek, J., Alimgazinova, N.Sh., Kyzgarina, M.T., and Atamurat, A.B. N22 shan kopirshikteri zhanyndagy zhas zhuldyz obektilerin anyqtau. Izvestija Nacional'noj Akademii Nauk Respubliki Kazahstan. Serija Fiz-Mat, 3 (337), 96–105 (2021). (in Kazakh). https://doi.org/10.32014/2021.2518-1726.51

7 Nazar, A.B., Manapbaeva, A.B., Alimgazinova, N.Sh., Kyzgarina, M.T., and Demessinova, A.M. Identification of young star objects near dust bubble N10. Recent Contributions to Physics, 4 (83), 13–20 (2022). https://doi.org/10.26577/RCPh.2022.v83.i4.02

8 Alimgazinova, N.Sh., Sharipbay, N.A., Kyzgarina, M.T., Manapbaeva, A.B., Turekhanova, K.M., Omar, A.Zh., Demessinova, A.M., and Alibek, A.A. Study of the N126 dust bubble in the infrared wavelength range. Recent Contributions to Physics, 2, 19–26 (2024). https://doi.org/10.26577/RCPh.2024v89i2-03

9 Alimgazinova, N.Sh. Young stellar objects in the region of dust bubble N1. Recent Contributions to Physics, 1 (92), 50–60 (2025). https://doi.org/10.26577/RCPh20259215

10 Reipurth, B., et al. Handbook of Star Forming Regions. Volume I: The Northern Sky (San Francisco, CA: Astronomical Society of the Pacific, 2008), 1023 p. ISBN: 978-1-58381-670-7

11 Komesh, T., Esimbek, J., Baan, W., Zhou, J., Li, D., Wu, G., He, Y., Sailanbek, S., Tang, X., and Manapbayeva, A. H_2CO and H110α observations toward the Aquila Molecular Cloud. The Astrophysical Journal, 874 (2), 172 (2019). https://doi.org/10.3847/1538-4357/ab0ae3

12 Tursun, K., Esimbek, J., Henkel, C., Tang, X., Wu, G., Li, D., et al. Ammonia observations towards the Aquila Rift cloud complex. Astronomy & Astrophysics, 643, A178 (2020). https://doi.org/10.1051/0004-6361/202037659

13 Komesh, T., Baan, W., Esimbek, J., Zhou, J., Li, D., Wu, G., He, Y., Rosli, Z., and Ibraimov, M. Studies of the distinct regions due to CO selective dissociation in the Aquila molecular cloud. Astronomy & Astrophysics, 644, A46 (2020). https://doi.org/10.1051/0004-6361/202038632

14 Bontemps, S., et al. The Herschel first look at protostars in the Aquila Rift. Astronomy & Astrophysics, 518, L85 (2010). https://doi.org/10.1051/0004-6361/201014661

15 Kirk, H., Myers, P.C., Bourke, T.L., et al. Filamentary accretion flows in the embedded Serpens South protocluster. Astrophysical Journal, 766 (2), 115 (2013). https://doi.org/10.1088/0004-637X/766/2/115

16 Könyves, V., André, P., Men'shchikov, A., et al. A census of dense cores in the Aquila Cloud Complex: SPIRE/PACS observations from the Herschel Gould Belt Survey. Astronomy & Astrophysics, 584, A91 (2015). https://doi.org/10.1051/0004-6361/201525861

17 Straižys, V., Černis, K., and Bartašiūtė, S. Interstellar extinction in the direction of the Aquila Rift. Astronomy & Astrophysics, 405 (2), 585–590 (2003). https://doi.org/10.1051/0004-6361:20030599

18 Dzib, S., et al. VLBA determination of the distance to nearby star-forming regions. IV. A preliminary distance to the proto-Herbig Ae/Be star EC 95 in the Serpens Core. Astrophysical Journal, 718 (2), 610–619 (2010). https://doi.org/10.1088/0004-637X/718/2/610

19 Ortiz-León, G.N., Dzib, S.A., and Kounkel, M.A. The Gould's Belt Distances Survey (GOBELINS). Astrophysical Journal, 834 (2), 143 (2017). https://doi.org/10.3847/1538-4357/834/2/143

20 Ortiz-León, G.N., Loinard, L., Dzib, S.A., et al. Gaia-DR2 confirms VLBA parallaxes in Ophiuchus, Serpens, and Aquila. Astrophysical Journal Letters, 869 (2), L33 (2018). https://doi.org/10.48550/arXiv.1812.02360

21 Anderson, A.R., Williams, J.P., van der Marel, N., et al. Protostellar and protoplanetary disk masses in the Serpens region. Astrophysical Journal, 938 (1), 55 (2022). https://doi.org/10.48550/arXiv.2204.08731

22 André, P., Men'shchikov, A., et al. From filamentary clouds to prestellar cores to the stellar IMF: Initial highlights from the Herschel Gould Belt Survey. Astronomy & Astrophysics, 518, L102 (2010). https://doi.org/10.1051/0004-6361/201014666

23 Pokhrel, R., Megeath, S.T., et al. Extension of HOPS out to 500 pc (eHOPS). I. Identification and modeling of protostars in the Aquila molecular clouds. Astrophysical Journal Supplement Series, 266 (2), 32 (2023). https://doi.org/10.3847/1538-4365/acbfac

24 Spitzer Heritage Archive. Available at: http://sha.ipac.caltech.edu/applications/Spitzer/SHA (accessed March 13, 2026).

25 Smith, J., et al. Infrared sources and excitation of the W40 complex. Astrophysical Journal, 291, 571–580 (1985). https://doi.org/10.1086/163097

26 Komesh, T., Garay, G., Henkel, C., Omar, A., Estalella, R., Assembay, Z., et al. Infall motions in the hot core associated with the hypercompact H II region G345.0061+01.794 B. The Astrophysical Journal, 967 (1), 15 (2024). https://doi.org/10.3847/1538-4357/ad3e7b

27 Shen, H., Esimbek, J., Henkel, C., Li, D.L., Zhou, J.J., He, Y.X., Tang, X.D., Wu, G., Komesh, T., Tursun, K., Zhou, D.D., Ma, Y., Sailanbek, S., and Berdikhan, D. Triggered and dispersed under feedback of super H II region W4. Astronomy & Astrophysics, 693, A21 (2025). https://doi.org/10.1051/0004-6361/202450914

28 Omar, A., Abdirakhman, A., Alimgazinova, N., Kyzgarina, M., Naurzbayeva, A., Islyam, Z., Turekhanova, K., Demessinova, A., and Manapbayeva, A. ALMA Observations of G333.6–0.2: Molecular and Ionized Gas Environment. Galaxies, 13 (4), 73 (2025). https://doi.org/10.3390/galaxies13040073

29 Pirogov, L., et al. Molecular-line and continuum study of the W40 cloud. Monthly Notices of the Royal Astronomical Society, 436, 3186–3199 (2013). https://doi.org/10.1093/mnras/stt1802

30 Su, Y., et al. Local molecular gas toward the Aquila Rift region. Astrophysical Journal, 893 (2), 91 (2020). https://doi.org/10.3847/1538-4357/ab7fff

31 Mallick, M., et al. The W40 region in the Gould Belt: An embedded cluster and H II region at the junction of filaments. Astrophysical Journal, 779 (2), 113 (2013). https://doi.org/10.1088/0004-637X/779/2/113

32 VizieR Catalog. URL: https://vizier.cds.unistra.fr/viz-bin/VizieR?-source=II/246 (accessed March 13, 2026).

33 AllWISE Data Release (Cutout). URL: https://vizier.cds.unistra.fr/viz-bin/VizieR-3?-source=II/328/allwise (accessed March 13, 2026).

34 Kang, S.-J., Kerton, C.R., Choi, M., and Kang, M. A comparative observational study of YSO classification in four small star-forming H II regions. Astrophysical Journal, 845 (1), 21 (2017). https://doi.org/10.3847/1538-4357/aa7da3

35 Koenig, X.P., and Leisawitz, D.V. A classification scheme for young stellar objects using the Wide-field Infrared Survey Explorer AllWISE catalog: revealing low-density star formation in the outer Galaxy. Astrophysical Journal, 791 (2), 131 (2014). https://doi.org/10.1088/0004-637X/791/2/131

36 Greene, T.P., Wilking, B.A., André, P., Young, E.T., and Lada, C.J. Further mid-infrared study of the ρ Ophiuchi cloud young stellar population: Luminosities and masses of pre-main-sequence stars. Astrophysical Journal, 434, 614–626 (1994). https://doi.org/10.1086/174763

37 SIMBAD Astronomical Database. URL: https://simbad.u-strasbg.fr/simbad/ (accessed March 13, 2026).

38 NASA/IPAC Infrared Science Archive (IRSA). URL: https://irsa.ipac.caltech.edu/frontpage/ (accessed March 13, 2026).

39 Komesh, T., et al. ALMA observations of the environments of G333.0162+00.7615. Proceedings of the International Astronomical Union, 17 (S373), 35–38 (2021). https://doi.org/10.1017/S1743921323000121

40 Assembay, Z., et al. ALMA observations of the environments of G301.1364-00.2249 A. Proceedings of the International Astronomical Union, 18 (S380), 204–206 (2022). https://doi.org/10.1017/S1743921323002624

41 Pokhrel, R., Megeath, S.T., Gutermuth, R., et al. Extension of HOPS out to 500 parsecs (eHOPS). I. Identification and modeling of protostars in the Aquila molecular clouds. Astrophysical Journal Supplement Series, 266 (2), 32 (2023). https://doi.org/10.48550/arXiv.2209.12090

42 Abdullayev, Z., Komesh, T., Grossan, B., Abdikamalov, E., Maksut, Z., Krugov, M., Myrzakul, S., et al. Early-time optical spectral shape measurements of GRB 200925B. Revista Mexicana de Astronomía y Astrofísica (Serie de Conferencias), 59, 109–113 (2025). https://doi.org/10.22201/ia.14052059p.2025.59.20

43 Könyves, V. The Aquila prestellar core population revealed by Herschel. Astronomy & Astrophysics, 518, L106 (2010). https://doi.org/10.1051/0004-6361/201014689

44 Strom, K.M., Strom, S.E., Edwards, S., Cabrit, S., Skrutskie, M.F., et al. Circumstellar material associated with solar-type pre-main-sequence stars: A possible constraint on the timescale for planet building. Astronomical Journal, 97 (5), 1451–1470 (1989). https://doi.org/10.1086/115085

45 Marton, G., Verebélyi, E., Kiss, C., and Smidla, J. Newly identified YSO candidates towards the LDN 1188. Astronomische Nachrichten, 334 (9), 924–927 (2013). https://doi.org/10.1002/asna.201311960

46 Straižys, V., Černis, K., and Bartasiūtė, S. Interstellar extinction in the direction of the Aquila Rift. Astronomy & Astrophysics, 405 (2), 585–590 (2003). https://doi.org/10.1051/0004-6361:20030599

47 Robitaille, V.P., Whitney, B.A., Indebetouw, R., Wood, K., and Denzmore, P. Interpreting spectral energy distributions from young stellar objects. II. Fitting observed SEDs using a large grid of precomputed models. Astrophysical Journal Supplement Series, 169 (2), 328–352 (2007). https://doi.org/10.1086/512039

[1,2]Алимгазинова Н.Ш.,
ф-м.ғ,к., ORCID ID: 0000-0002-4596-1855,
e-mail: Nazgul.Alimgazinova@kaznu.kz
[2,3]Манапбаева А.Б.,
PhD, ORCID ID: 0000-0002-0322-1509,
e-mail: manapbayeva.arailym@gmail.com
[1,2]*Омар А.Ж.,
PhD, ORCID ID: 0000-0002-5604-3742,
*e-mail: omaruzhan@gmail.com
[1,2]Демесинова А.М.,
PhD, ORCID ID:0000-0001-5049-9338,
e-mail:aizat.dem@gmail.com
[1,2]Туреханова К.М.,
ф-м.ғ,к., ORCID ID:0000-0003-4662-7290,
e-mail: kunduz@physics.kz
[1]Абилдаев Н.Е.
ORCID ID: 0009-0009-1934-4907,
e-mail: nurlanabildaev833@gmail.com.

[1]Әл-Фараби атындағы Қазақ ұлттық университеті, Алматы қ., Қазақстан,
[2]Әл-Фараби атындағы Қазақ ұлттық университетінің Эксперименттік
және теориялық физика институты, Алматы қ., Қазақстан,
[3]Қазақ ұлттық қыздар педагогикалық университеті, Алматы қ., Қазақстан

W40 ЖҰЛДЫЗ ТҮЗІЛУ АЙМАҒЫН WISE ИНФРАҚЫЗЫЛ ҒАРЫШТЫҚ ТЕЛЕСКОПЫ БАҚЫЛАУЛАРЫМЕН ЗЕРТТЕУ

Аңдатпа

Жұлдыздардың түзілуі мен эволюциясының механизмдерін зерттеу мен жас жұлдызды нысандарды (ЖЖН) анықтау – жұлдызаралық ортаның аймақтарын кешенді түрде қарастыруға негізделеді. Жас жұлдызды нысандардың сәулеленуін, инфрақызыл аралығының әртүрлі толқын ұзындықтары арқылы идентификациялау, салыстырмалы түрде жаңа бағыт. Бұл бағыттағы алғашқы зерттеулер XX ғасырдың соңында ғана пайда болды. Бақылау техникасы, деректерді өңдеу әдістері, жұлдызды көздердің физикалық сипаттамаларын анықтаудың сенімді әдістері мен ғарыштағы нысандар туралы көлемді ақпарат массивтерінен тұратын каталогтардың құрылуымен, осы бағыттың дамуы мүмкін болды. Бұл жұмыс Aquilla молекулалық бұлтында орналасқан W40 жұлдыз түзілу аймағынан эволюцияның әртүрлі кезеңіндегі бұрын анықталмаған жас жұлдызды нысандарды анықтау мен оларды тіркеу әдістерінің инфрақызыл зерттеулеріне арналған. Идентификациялау екі әдіс бойынша жүргізілді: фотометриялық алғышарттар мен спектралды индекстер негізінде. Бұл тәсілдер жас жұлдыздарға үміткер болатын 37 бұрын зерттелмеген жаңа нысанды және олардың эволюциялық кезеңдерін (5 нысан – I класс, 2 нысан – II класс, 4 нысан – «өтпелі дискілер» класы және 26 нысан – III класс) сенімді түрде анықтауға мүмкіндік берді. Алынған нәтижелер W40 аймағында жұлдыз түзілу құбылыстарының белсенді түрде жалғасып жатқанын көрсетеді.

Тірек сөздер: W40 жұлдыз түзілу аймағы, инфрақызыл сәулелену, WISE, жас жұлдызды нысандар, эволюциялық кезең.

[1,2]Алимгазинова Н.Ш.,
к.ф-м.н., ORCID ID: 0000-0002-4596-1855,
e-mail: Nazgul.Alimgazinova@kaznu.kz
[2,3]Манапбаева А.Б.,
PhD, ORCID ID: 0000-0002-0322-1509,
e-mail: manapbayeva.arailym@gmail.com
[1,2]*Омар А.Ж.,
PhD, ORCID ID: 0000-0002-5604-3742,
*e-mail: omaruzhan@gmail.com
[1,2]Демесинова А.М.,
PhD, ORCID iD:0000-0001-5049-9338,
e-mail:aizat.dem@gmail.com
[1,2]Туреханова К.М.,
к.ф-м.н., ORCID iD:0000-0003-4662-7290,
e-mail: kunduz@physics.kz
[1]Абилдаев Н.Е.
ORCID iD: 0009-0009-1934-4907,
e-mail: nurlanabildaev833@gmail.com.

[1]Казахский национальный университет им. аль-Фараби, г. Алматы, Казахстан,
[2]Институт экспериментальной и теоретической физики,
Казахский национальный университет им. аль-Фараби, г. Алматы, Казахстан,
[3]Казахский национальный женский педагогический университет, г. Алматы, Казахстан

ИССЛЕДОВАНИЕ ОБЛАСТИ ЗВЕЗДООБРАЗОВАНИЯ W40 НА ОСНОВЕ НАБЛЮДЕНИЙ ИНФРАКРАСНОГО КОСМИЧЕСКОГО ТЕЛЕСКОПА WISE

Аннотация

Изучение механизмов образования и эволюции звезд основано на комплексных исследованиях областей межзвездной среды, включая анализ и идентификацию молодых звездных объектов (МЗО). Идентификация молодых звездных объектов по их излучению на различных длинах волн инфракрасного диапазона ведется относительно недавно – первые исследования в этой области появились лишь в конце XX века. Развитие данного направления стало возможным благодаря совершенствованию наблюдательной техники и методов обработки данных, получению более надежных характеристик звездных источников, а также созданию каталогов, содержащих обширные массивы информации о космических объектах. В данной работе было проведено исследование области звездообразования W40 молекулярного облака Aquilla в инфракрасном диапазоне длин волн на предмет обнаружения ранее не идентифицированных и находящихся на различных стадиях эволюции молодых звездных объектов. Идентификация проводилась с использованием двух подходов: по фотометрическим критериям и спектральномым индексам. Это позволило более достоверно выявить эволюционные стадии впервые найденных и ранее неисследованных 37 кандидатов в МЗО (5 объектов – I класса, 2 объекта – II, 4 объекта – класса «переходные диски» и 26 объектов – III класса), что свидетельствует об активном и продолжающемся процессе звездообразования в W40.

Ключевые слова: область звездообразования W40, инфракрасное излучение, WISE, молодые звездные объекты (МЗО), эволюционная стадия.